Macromolecular Chemistry and Physics
www.mcp-journal.de

Influence of Carbon Dioxide on the Phase Behavior of Pharmaceutical Drug-Polymer Dispersions

*Jana Klueppelberg, Ulrich A. Handge, Markus Thommes, and Judith Winck**

The formulation as amorphous solid dispersion (ASD) addresses recent challenges in the oral administration of poorly-soluble drugs by embedding them in highly-soluble carrier polymers. In this context, utilizing CO_2 as a processing agent is an innovative strategy to facilitate the dissolution of the drug in the polymer at comparatively low temperatures without the use of any organic solvents. Within this study, the influence of CO_2 on the phase behavior of ASD formulations is investigated. Therefore, high-pressure differential scanning calorimetry is applied to evaluate the dissolution of the drugs in the polymers and the glass transition temperatures under CO_2 of four formulations containing the drugs acetaminophen and itraconazole as well as the polymers Soluplus and vinylpyrrolidone/vinyl acetate copolymer. The glass transition temperatures of the ASD formulations decrease with CO_2 fraction dissolved in the polymer. The extent of T_g reduction is related to the spatial structure and intermolecular interactions of the polymers. Furthermore, the sorption of CO_2 accelerates the diffusion of the drugs in the plasticized polymers. However, phase separation is observed in some formulations under CO_2 loading which has an impact on the stability of the ASD and has to be considered in process design.

1. Introduction

The formation of amorphous solid dispersions (ASD) is a promising technique in pharmaceutical applications to overcome the low bioavailability of orally administered drugs.[1] According to that, the solubility of drugs is increased by molecularly dispersing them in amorphous and highly soluble carrier polymers. The advantages of manufacturing ASD formulations by hot melt extrusion (HME) are the solvent-free production method, the possibility to easily scale up the process, and the potential to be implemented in a continuous process.[2] A major disadvantage, on the other hand, is the high process temperatures that are required to plasticize the polymer and dissolve the drug in a molecularly dispersed form.[3] The temperature-sensitive drug can subsequently degrade and, in addition to reduced effectiveness, form decomposition products that are harmful to the patient's health.[4]

One way to reduce the required temperatures during polymer extrusion is to use carbon dioxide (CO_2) as a plasticizing agent.[5,6] The molecules diffuse into the polymer, increasing the free volume between the polymer chains and allowing plastification at lower temperatures.[7] This effect is more pronounced with increasing hydrostatic pressure. CO_2 is particularly suitable as a swelling gas, as its chemical structure facilitates a high solubility in most polymers.[8] It is used in many process engineering applications as a largely inert and non-toxic substance.[9] Accordingly, CO_2 is in particular suitable for use in pharmaceutical technology and can be removed from the product without any harmful residues by subsequent decompression.[10]

In ASD manufacturing, CO_2–assisted extrusion of various drug-polymer systems showed less degradation of the product[11] and faster drug release,[12] which can be explained by the increased surface area of the porous extrudates.[13] The porous structure also improved the further processing of the extrudates, since during the subsequent grinding, higher efficiency and comparatively small particle sizes can be achieved with lower energy input.[14a,b,16] Furthermore, the hardness and tensile strength of tablets produced on the basis of porous extrudates are increased and their friability is reduced.[15,17] In storage tests, the products extruded with CO_2 showed the same stability as extrudates processed without.[16]

Another application of CO_2 in the preparation of ASD formulations is the impregnation of polymers with drugs, using supercritical CO_2 ($scCO_2$) as a transport agent.[18] The dissolved CO_2 increases the free volume and enhances the chain mobility so that it facilitates the diffusion of the drug through the polymer. As an example, various commonly used pharmaceutical excipient polymers were successfully impregnated with the drugs ibuprofen,[19] indomethacin,[20] and carvedilol[21] far below temperatures that are reasonably necessary for solvent-free

J. Klueppelberg, M. Thommes, J. Winck
Laboratory of Solids Process Engineering
TU Dortmund University
Emil-Figge-Str. 68, 44227 Dortmund, Germany
E-mail: judith.winck@tu-dortmund.de
U. A. Handge
Chair of Plastics Technology
TU Dortmund University
Leonhard-Euler-Str. 5, 44227 Dortmund, Germany

The ORCID identification number(s) for the author(s) of this article can be found under https://doi.org/10.1002/macp.202400359

DOI: 10.1002/macp.202400359

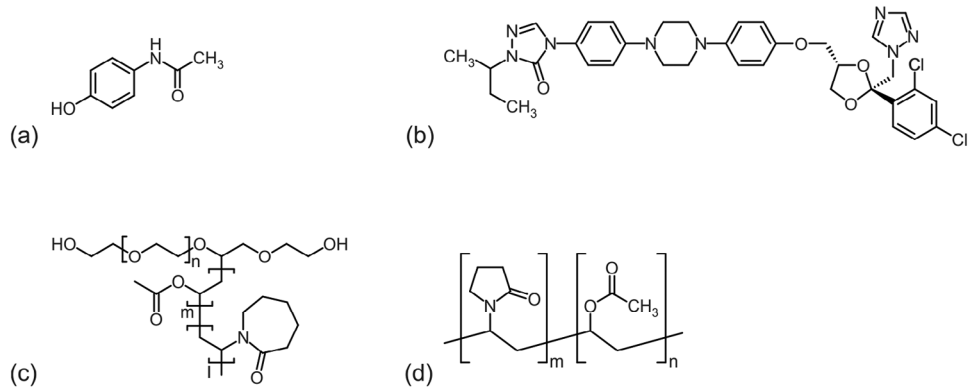

Figure 1. Molecular structure of drugs a) acetaminophen, b) itraconazole and polymers c) Soluplus d) vinylpyrrolidone/vinyl acetate copolymer.

processing, using $scCO_2$ technology. Although the application studies highlight the potential of optimizing solvent-free ASD processing through utilizing CO_2 as a processing agent, there is a lack of fundamental knowledge concerning the effect of pressurized CO_2 on the interaction and phase behavior of polymer and drug.

The phase behavior of an ASD is usually evaluated based on phase diagrams that present the solubility temperature of the crystalline drug in the polymer and the glass transition temperature of the ASD depending on the drug weight fraction.[22,23] Here, the solution equilibrium of a crystalline drug in a polymer describes the state in which the chemical potential for constant pressure and temperature in the solid phase is equal to the chemical potential in the liquid phase. The glass transition of an amorphous polymer-drug solution describes the temperature range that characterizes the transition from the glassy state at low temperatures to the rubbery state at higher temperatures which is associated with an increased molecular mobility.

So far, no studies have been published about the effect of CO_2 loading on the solubility temperature of drugs in polymers and how the glass transition temperatures change in these ternary systems. Therefore, it is of particular interest to investigate the phase behavior of polymer-drug systems under CO_{2-} pressure to draw conclusions about intermolecular interactions that are relevant for process design and product performance. In this study, the effect of CO_2 on the phase behavior of pharmaceutical polymer-drug dispersions is investigated with regard to the solubility and glass transition temperatures using high-pressure differential scanning calorimetry (HP-DSC). Phase diagrams of four polymer-drug formulations are evaluated at various CO_{2-} pressures, representing different states of gas sorption, in order to interpret the ternary systems. Based on the proposed methodology of considering varying heating rates in HP-DSC, kinetic effects as the diffusivity are extracted from the data representing the equilibrium state and assessed separately.

2. Experimental Section

2.1. Materials

Two model drugs were selected to prepare ASD formulations with two commonly used amorphous excipient polymers, respectively (**Figure 1**).

Table 1. Material data of drugs and polymers.

Substance	M_w [g/mol]	ρ_{true} [g/cm^3]	Δh_m [J/g]	T_g[°C]	T_m[°C]
ACE	151.2[a)]	1.29[b)]	179.2	22.5	170.0
ITR	705.6[c)]	1.27[d)]	85.8	57.6	164.9
SOL	118 000[e)]	1.08[f)]	–	78.2	–
PVPVA	57 500[e)]	1.19[f)]	–	109.0	–

[a)] Lehmkemper et al.[24] [b)] Nair et al.[25] [c)] Wolbert et al.[26] [d)] Six et al.[27] [e)] Altamimi and Neau[28] [f)] Gottschalk et al.[29]

The drugs Acetaminophen (ACE) (Caelo, Caesar & Loretz GmbH, Hilden, Germany) and Itraconazole (ITR) (BASF SE, Ludwigshafen, Germany) differ in their molecular weight whereas exhibiting similar melt temperatures (**Table 1**). Furthermore, as polymers a vinylpyrrolidone-vinyl acetate copolymer (PVPVA) Kollidon VA64 (BASF SE) and an ethylene glycol- vinylcaprolactam-vinyl acetate copolymer Soluplus (SOL) (BASF SE) were selected.

2.2. High-Pressure Differential Scanning Calorimetry

Calorimetric measurements were performed under elevated pressure in a CO_2 atmosphere to determine characteristic temperatures of the phase diagrams using a high-pressure DSC 204 HP Phoenix (NETZSCH-Gerätebau GmbH, Selb, Germany). Prior to the measurements, physical polymer-drug powder mixtures were ground in order to reduce the average particle size and generate intimate contact so that complete dissolution of the drug in the polymer is achieved during the heating cycle in the HP-DSC apparatus. Therefore, formulations containing ACE were ground at 50 Hz for 9 min in three cycles using a Pulverisette 23-ball mill (Fritsch GmbH, Idar-Oberstein, Germany). For formulations containing ITR, a SPEX CertiPrep 6850 cryomill (SPEX CertiPrep, Metuchen, USA) was utilized at 10 Hz for 16 min in 8 circles since ITR tended to aggregate during ball milling. For each measurement, Concavus sample crucibles (NETZSCH-Gerätebau GmbH) were filled with a sample of mass between 7 and 15 mg and sealed with the crucible press. The crucible lids were perforated with three holes, respectively, in order to allow a sufficient change of atmosphere in the crucible.

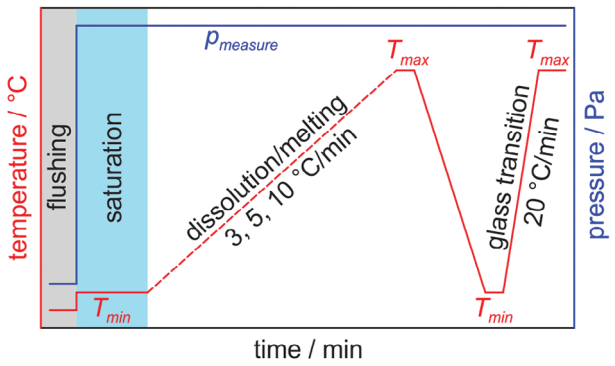

Figure 2. A heating protocol was applied to determine the solubility temperature of the crystalline drug in the polymer and the glass transition temperature of the ASD at elevated pressure.

The measuring cell was continuously purged with CO_2 at a flow rate of 180 mL min^{-1}.

The heating and pressurization protocol was adopted in a way to evaluate both, the solubility temperature of the crystalline drug in the polymer and the glass transition temperature of the ASD (**Figure 2**). After placing the sample crucible in the measuring cell, it was flushed with CO_2 for 5 min to remove the remaining air. This was followed by a saturation step for the CO_2 sorption at elevated pressure. The saturation was performed at T_{min}, i.e. 50 °C below the glass transition temperature of the polymer for 60 min which was assessed as sufficient for the CO_{2-} sorption of the finely ground powder.[30] The sample was then heated to T_{max}, i.e. 50 °C above the melting temperature of the drug. The heating rate was varied from 3 to 5 to 10 °C min^{-1} in order to subsequently extrapolate the measuring data linearly to a zero heating rate to be able to determine the phase equilibrium of crystalline drug and polymer based on the endpoints of melting from the melting point depression method.[23,31] After a holding time of 10 min, the sample was cooled down to T_{min} at 10 °C min^{-1}. This was followed by a 15 min isothermal segment. Finally, the sample was heated at 20 °C min^{-1} to analyze the glass transition temperature of the ASD according to the inflection point method.[32]

3. Results and Discussion

3.1. Solubility of Drugs in Polymers under Carbon Dioxide

The solubility temperatures of drug-polymer systems are equivalent to the depressed melting points of the crystalline drug in the polymer at specific drug weight fractions. In this context, the solubility temperature decreases with increasing polymer fraction in a drug-polymer system as shown exemplarily in the DSC thermograms for the ACE/PVPVA formulation in **Figure 3**, left. Furthermore, there is a clear trend from a sharp melting peak of the pure drug to broader peaks for increasing polymer fractions. This is attributed to a shift from a melting process to the dissolution of the drug in the polymer which already is initiated at temperatures lower than the melting temperature and is characterized by mass transport phenomena.

The comparative presentation of HP-DSC thermograms at 1 and 4 MPa CO_{2-} pressure (Figure 3, right) shows the effect of the CO_2 fraction on the dissolution of the crystalline drug in the polymer. All HP-DSC measurements were performed in the subcritical region of CO_2, as the supercritical state is only reached at 7.4 MPa. The dissolution peaks of ACE in PVPVA are shifted to lower temperatures and appear flatter with increasing CO_{2-} pressure. This implies that the CO_2 is dissolved in the drug-polymer system, which, in turn, influences the dissolution of the drug in the polymer. However, when comparing the HP-DSC measurements at a heating rate of 10 °C min^{-1}, the thermograms could be overlaid by kinetic effects. This is attributed to the fact that dissolved CO_2 accelerates the diffusion of small molecules, such as drugs, in polymers and the strength of this effect differs with the fraction and pressure of the gas.[33] In order to remove the impact of this kinetic effect and to make the data at different CO_{2-} pressures comparable, all solubility temperatures are presented hereinafter at a theoretical heating rate of 0 °C min^{-1} to represent the equilibrium state. Therefore, the end of melting, measured at three different heating rates, is linearly extrapolated to a zero heating rate to obtain the solubility temperatures (**Figure 4**, left).

The solubility temperatures of the drug-polymer system ACE in PVPVA are depicted in Figure 4, right. The melting temperature of the pure drug does not show a dependency on the CO_{2-}

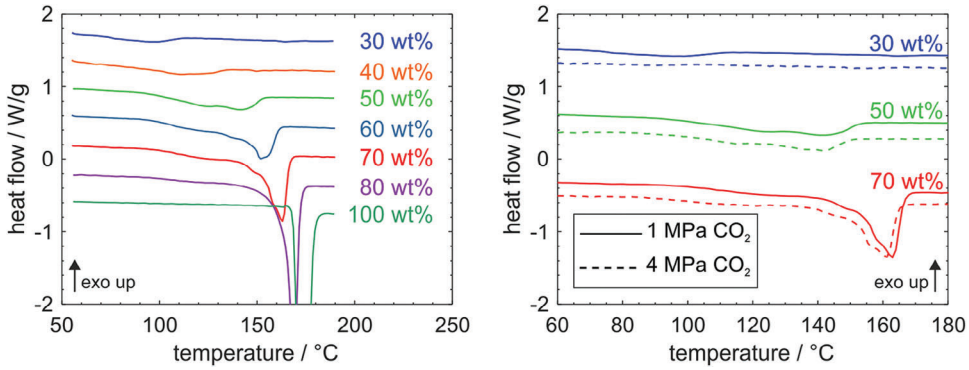

Figure 3. HP-DSC thermograms of the drug dissolution/melting of ACE/PVPVA with drug weight fractions of 30 to 100 wt.% at 1 MPa CO_{2-} pressure and a heating rate of 10 °C min^{-1} (left). HP-DSC thermograms of the drug dissolution/melting of ACE/PVPVA with drug weight fractions of 30, 50, and 70 wt.% at 1 and 4 MPa CO_{2-} pressure and a heating rate of 10 °C min^{-1} (right).

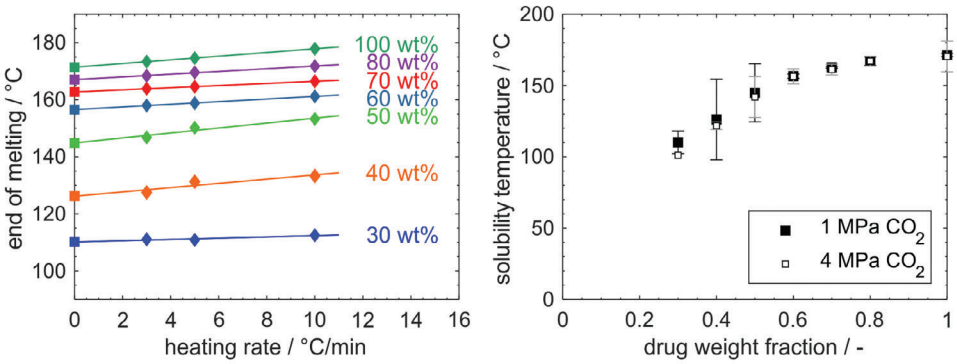

Figure 4. End of melting temperatures of ACE/PVPVA at 1 MPa $CO_{2\_}$ pressure measured at three different heating rates (diamonds), linearly extrapolated to a zero heating rate (squares) (left). Solubility temperatures of ACE/PVPVA depend on the drug weight fraction and the $CO_{2\_}$ pressure (right). Error bars represent confidence intervals (significance level $\alpha = 0.05$) for the solubility temperature when extrapolating the three different heating rates to a zero heating rate (see Section S.1, Supporting Information).

pressure when taking into account measurement uncertainties. It is thus concluded that the dissolution of CO_2 in the crystalline drug is negligibly small under the experimental conditions considered in this study so that no depression of the melting point was observed.

The solubility of the drugs in compressed CO_2 highly depends on pressure and temperature, while there are significant differences between the subcritical and supercritical states.[34] However, literature data on the solubility of the drugs used in this study in compressed CO_2 is only available for the supercritical state above 7.4 MPa.[35] Consequently, the solubility of ACE and ITR in subcritical CO_2 at 1 and 4 MPa is not known.

For the formulations containing drug and polymer, the solubility temperatures shift to lower temperatures with increasing pressure. The extent of the effect depends on the polymer fraction of the formulation. If the fraction of PVPVA increases, the reduction in the solubility temperatures between 1 and 4 MPa $CO_{2\_}$ pressure also increases. At 70 wt.% polymer, the solubility temperature is reduced from 110 °C at 1 MPa to 101 °C at 4 MPa. However, statistically significant differences between 1 and 4 MPa values could not be observed due to the comparatively high uncertainty of HP-DSC measurements (see Section S.1, Supporting Information).

The reduction of the solubility temperature in drug-polymer formulations is related to the dissolution of CO_2 in the polymer fraction at elevated pressure. With a larger amount of polymer and a higher pressure, more CO_2 is dissolved in the drug-polymer formulation. The dissolved CO_2 in turn promotes the dissolution of a larger amount of drug in the polymer. It is concluded that the dissolving CO_2 creates additional cavities in the polymer, associated with an increase in free volume as well as a higher mobility of the polymer chains. Due to the high affinity of ACE to PVPVA,[36] this free volume in the polymer is subsequently occupied by the drug molecules. This mechanism is already known in the context of $CO_{2\_}$ assisted impregnation of polymers with additives. Even if an additive is not sufficiently soluble in CO_2 to be transported directly with the CO_2 phase into the polymer, a successful impregnation is achieved via partitioning of the additive between polymer and CO_2 phases in case of a high affinity of the additive to the polymer.[33,37]

3.2. Glass Transition of Amorphous Solid Dispersions under Carbon Dioxide

In case the drug is completely dissolved in the polymer during the first DSC heating cycle, a single glass transition is found in the thermograms of the second heating cycle (**Figure 5**, left). This glass transition temperature of the ASD is then located between the glass transition temperatures of pure drug and polymer.

The glass transition of the ASD formulations is shifted to lower temperatures by increasing the $CO_{2\_}$ pressure from 1 to 4 MPa (Figure 5, right). Depending on the ASD composition, differences in this decrease of the glass transition temperature are recognizable. For higher polymer fractions, the effect of the $CO_{2\_}$ pressure is stronger which is attributed to the higher dissolution of the CO_2 in the polymer and the resulting plastification. The gas diffuses into the intermolecular spaces, contributing to the spatial separation of the polymer chains and thus ensuring greater mobility at relatively low temperatures.[38] Particularly in the case of polar polymers, the mobility of the chain segments can also be restricted by dipole forces. The dissolved CO_2 interacts as a Lewis acid with the functional groups of the polymer.[39] Hydroxyl, ether, and carbonyl groups seem to interact predominantly with the molecule as electron donors. As a result, the intramolecular interactions can be weakened, which further contributes to the plastification of the polymer.[5]

The decreasing glass transition temperatures of the ASD formulations were attributed primarily to the interaction of CO_2 with the polymer rather than the interaction with the drug. However, the glass transition temperatures of pure PVPVA and pure ACE were not accessible with the measurement setup used in this study. The HP-DSC apparatus was not equipped with a cooling unit so the glass transition temperature of ACE is too close to ambient temperature to be measured. When analyzing the pure polymer, the DSC signal of the glass transition is less pronounced at elevated $CO_{2\_}$ pressures and reaches finally the measurement limit. For other amorphous polymers, this limit was found in the range of 3 MPa.[40] Nevertheless, the reduction of the glass transition temperature of the ACE/PVPVA formulation under CO_2 was compared to literature data for pure PVPVA. At 30 wt.% drug weight fraction, the ASD glass transition is reduced by 13 °C

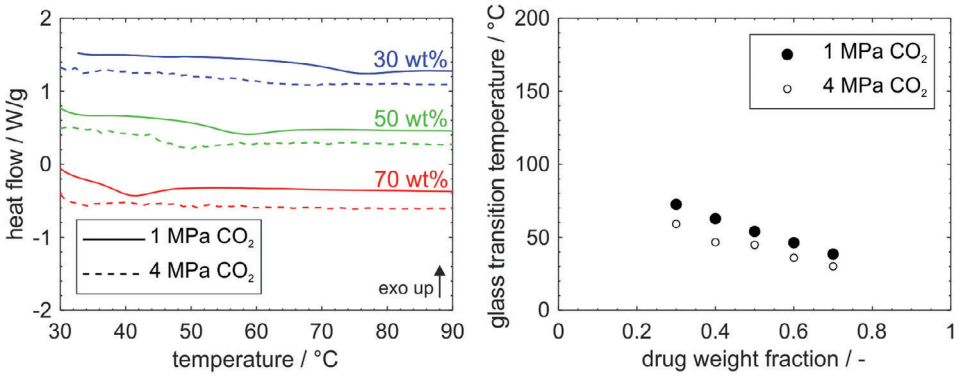

Figure 5. HP-DSC thermograms of the ASD glass transition of ACE/PVPVA with drug weight fractions of 30, 50, and 70 wt.% at 1 and 4 MPa CO_{2-} pressure (left). Glass transition temperatures of ASD formulations containing ACE/PVPVA depending on the drug weight fraction and the CO_{2-} pressure (right).

when increasing the CO_{2-} pressure from 1 to 4 MPa which is in good accordance with the reduction of 4.7 °C MP^{-1} measured for pure PVPVA in the pressure range of ambient to 6.1 MPa by Liu.[41]

3.3. Polymer-Drug Phase Diagrams under Carbon Dioxide

The effect of CO_2 on the solubility and glass transition temperatures of four drug-polymer formulations is evaluated based on the phase diagrams depicted in **Figure 6**. For comparison of the phase diagrams under 4 MPa CO_{2-} pressure (unfilled symbols), data from a previous study for measurements under nitrogen at atmospheric pressure are presented (filled symbols).[36]

In the first DSC heating cycle, the CO_{2-} pressure has no noticeable effect on the melting temperatures of the pure crystalline drugs ACE (Figure 6, top) and ITR (bottom). In the second heating cycle, the drug contains amorphous fractions formed in the preceding cooling step. CO_2 is dissolved in these amorphous fractions so that the glass transition temperature of ITR is slightly decreased. The glass transition temperature of pure ACE could not be measured under elevated CO_{2-} pressure as discussed in the previous section.

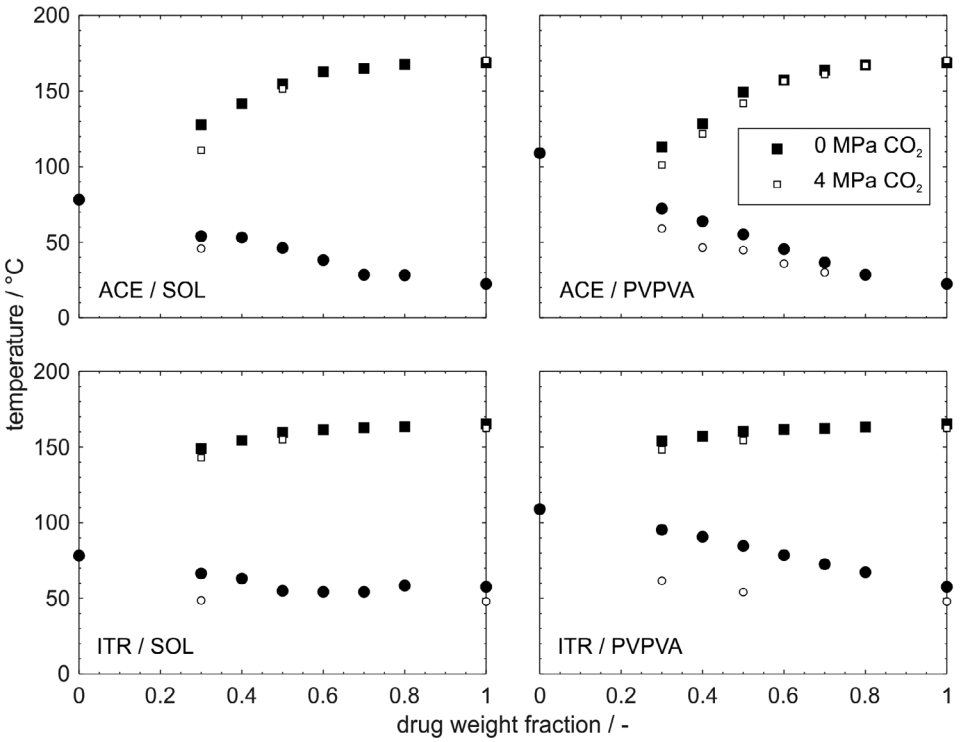

Figure 6. Solubility temperatures (squares) and glass transition temperatures (circles) of solid dispersions containing the drugs acetaminophen (top), itraconazole (bottom), and the polymers Soluplus (left), vinylpyrrolidone/ vinyl acetate copolymer (right). Data at 0 MPa CO_2 pressure is taken from the literature[36] for comparison with data at 4 MPa CO_2 pressure obtained within this study.

For all formulations containing drug and polymer, both the solubility and the glass transition temperatures are reduced at 4 MPa CO_{2-} pressure in comparison to the standard DSC measurements under a nitrogen atmosphere. The extent of the effect depends on the polymer content of the samples. As the fraction of polymer increases, the reduction in the characteristic temperatures also increases. This behavior is related to the stronger interaction of the polymer with CO_2, as described before.

The PVPVA formulations (right) show a higher decrease of the glass transition temperatures under CO_{2-} pressure in comparison to the SOL formulations (left). This is related to the spatial structure and intermolecular interactions of the polymers. Branching limits the mobility of the chains, but increases the number of end groups and free volume respectively which decreases the glass transition temperature.[42] In this context, it was also discussed by Li et al. that the solubility of CO_2 in a polymer and thus the swelling capacity can be lower for highly branched structures.[43] The reason lies in the limited solubility of the CO_2 due to the limited ability to increase the mass-specific volume. The increase in free volume and therefore the reduction of the glass transition temperature of the triblock graft polymer SOL seems to be limited due to its highly branched structure. In comparison, PVPVA is a slightly branched polymer with a linear structure and has only about half the molecular weight. The swelling of PVPVA due to the increase in free volume is therefore structurally less hindered. Accordingly, it seems evident that the change in the glass transition temperature with the CO_2 pressure is higher for the PVPVA formulations in comparison to the SOL formulations.

In addition to the different degrees of change in the glass transition temperature of the ASD formulations due to the choice of the polymer, there is also a correlation observed between the drug and the resulting intermolecular interactions. Larger shifts in the glass transition temperature under CO_2 are observed for the formulations containing ITR. The molecular weight of this drug is more than three times higher than that of ACE. Therefore, ITR is more subject to steric effects when interacting with and diffusing into other molecules.[44] Here, the swelling of the polymer by CO_2 can have a particularly strong effect on the plasticizing of the ASD formulations containing ITR. ACE, on the other hand, can arrange itself more easily in intermolecular spaces due to its comparatively small size. The effect of CO_2 on lowering the glass transition temperature seems to be limited as a result.

The decrease of the solubility temperature with the CO_{2-} pressure is more pronounced for the formulations containing the drug ACE. For ITR, only a slight effect of the CO_2 on the solubility temperatures was detected. Based on this, it is concluded that the change in glass transition temperature does not correlate with the change in solubility temperature of a formulation under CO_{2-} pressure. This can be observed in the fact that the glass transition temperature in formulations with ITR decreases more under CO_{2-} pressure, yet shows hardly any changes in solubility temperature. Conversely, the glass transition temperature in formulations with ACE decreases less compared to ITR, even though a greater change in solubility temperature is observed.

In the second DSC heating cycle, all formulations showed a single glass transition and no additional melting point of the remaining crystalline drug. It is concluded from this that a homogeneous and amorphous mixture was obtained for all formulations during the first heating cycle. This mixture is characterized by the single glass transition without any further processes seen in the HP-DSC thermograms. If no homogeneous mixture was formed, either a second glass transition would be visible if it was a second amorphous phase or a melting peak in the case of a crystalline phase. Furthermore, under the present measurement conditions in the subcritical region, practically no drug dissolves in CO_2.[34] From this, it is evident that the drug is completely embedded in the polymer. Accordingly, the final drug loading in the polymer matches the initially loaded fraction in the powder mixtures prepared for the HP-DSC measurements so both are referred to as drug weight fraction.

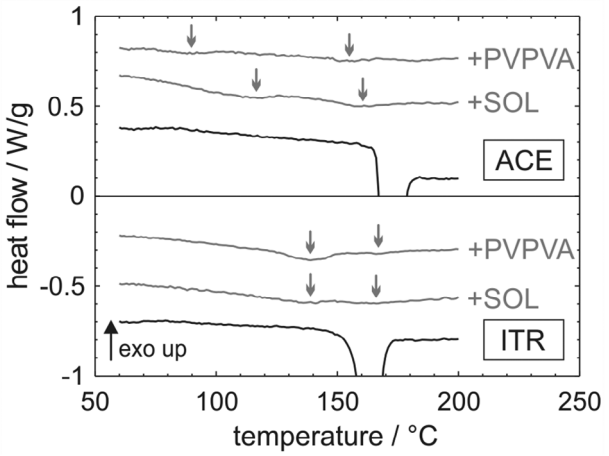

Figure 7. HP-DSC thermograms of the drug dissolution/melting of ACE and ITR as well as ASD formulations with drug weight fractions of 30 wt.% at 4 MPa CO_{2-} pressure and a heating rate of 10 °C min^{-1}.

When evaluating the HP-DSC thermograms of the first heating cycle in detail, it was observed that the dissolution peaks at low drug fractions of 30 wt.% appeared subdivided into two separate endothermic peaks under elevated CO_{2-} pressure (**Figure 7**). This indicates a phase separation where the drug is not molecularly dispersed in the polymer as expected for ASD formulations. Rather, in the phase-separated system, drug clusters are formed. Accordingly, the second endothermic peak in the HP-DSC thermograms at higher temperatures represents the melting of these drug clusters close to the melting temperature of the pure drug in the absence of the polymer. Consequently, the polymer matrix around the drug clusters contains less drug than originally weighed during the preparation of the formulation so that the solubility temperature shifts to lower temperatures in the phase diagram.

The outlined phase separation appears only if CO_2 is dissolved in the drug-polymer formulations and not in conventional DSC measurements under atmospheric conditions as known from a previous study.[36] The increase in free volume caused by the dissolved CO_2 facilitates the formation of the drug clusters. The second endothermic peak is very weak in the thermograms at 30 wt.% drug weight fraction. At higher drug fractions, both endothermic peaks are superimposed and cannot be separated from each other. For the construction of the phase diagrams (Figure 6), the end of both superimposed peaks was evaluated, except for the drug fractions of 40 wt.% and below where the first separated peak was evaluated. The ITR/SOL formulation with 30 wt.% drug

weight fraction showed a signal that was too weak to be analyzed at heating rates of 3 and 5 °C min^{-1} so for this formulation the data at 10 °C min^{-1} was combined with the slope of extrapolation at 50 wt.% drug weight fraction.

Finally, the finding that a miscibility gap in the ternary system under CO_2 can be formed, although the binary drug-polymer system is completely miscible, is crucial for the design of ASD manufacturing processes. Local supersaturation potentially causes nucleation and crystallization of the drug. As a result, the stability over a long storage time could be reduced. However, the drug-polymer phase behavior after CO_2 decompression has not yet been studied.

3.4. Influence of Carbon Dioxide on Polymer-Drug Interactions

In addition to the phenomena already described, it was observed that the area of the endothermic peak, i.e. the energy required to melt the drug or dissolve it in the polymer, decreases with increasing CO_2 pressure. When considering pure drugs, the associated melting enthalpy is a constant substance-specific value. However, in the present case, a ternary system of drug, polymer, and CO_2 is considered. Here, two superimposing dissolution processes occur. First, during the initial saturation step in the DSC, CO_2 dissolves in the polymer. Second, during the first heating, the drug dissolves in the polymer. As a result, the endothermic peak observed during the first heating characterizes the enthalpy change associated with the dissolution of the drug in the polymer. However, unlike in the scenario of a pure drug where the associated melting enthalpy remains constant, in the ternary system, the presence of CO_2 already dissolved in the polymer also influences the enthalpy change during the dissolution of the drug. Therefore, in the ternary system, a constant enthalpy cannot be assumed, as it is affected by both the drug and the dissolved CO_2. For further assessment of the underlying phenomena, the enthalpy change associated with the dissolution of the drug in the polymer (Δh_{diss}) when increasing the CO_{2-} pressure from 1 to 4 MPa is evaluated.

$$\Delta\left(\Delta h_{diss}\right) = \left(1 - \frac{\Delta h_{diss}\left(4\ MPa_{CO_2}\right)}{\Delta h_{diss}\left(1\ MPa_{CO_2}\right)}\right) \times 100\ \% \quad (1)$$

In **Figure 8**, the percentage change in enthalpy from 1 to 4 MPa CO_{2-} pressure is shown for the ACE/PVPVA formulation as a function of the drug weight fraction. The enthalpy change increases with increasing polymer fraction in the ASD. Since the dissolution of the CO_2 mainly takes place in the polymer, it can therefore be assumed that the decrease in the enthalpy under higher CO_{2-} pressure can be correlated with the CO_2 sorption. Dissolved CO_2 can cause a reduction in polarity and thus a weakening of the intermolecular interactions as investigated by Shukla et al. for deep-eutectic solvents.[45] A weakening of the hydrogen bonds of the crystalline drug would explain the decrease in the enthalpy.

3.5. Kinetic Effects on Drug Dissolution

In addition to the maximum fraction of drug that can be dissolved in the polymer, the rate of diffusion is another important parameter for describing the dissolution process. Therefore, the extrapolation of the end of melting temperatures (Figure 4, left) at 3, 5, and 10 °C min^{-1} to a zero heating rate is evaluated in more detail. The slope of the extrapolation represents the dependency of the diffusion on time. If the diffusion coefficient is low, the end of melting in the DSC thermogram only appears at much higher temperatures than the solubility temperature at equilibrium due to the limitation in mass transport, which delays the dissolution over time and thus the apparent temperature of the event during heating in the DSC. This effect is accordingly more pronounced, the higher the heating rate of the DSC. As a result, the slope of the extrapolation increases with a decrease of the diffusion rate. On the other hand, at an infinite high diffusion rate, the slope of the extrapolation approaches zero.

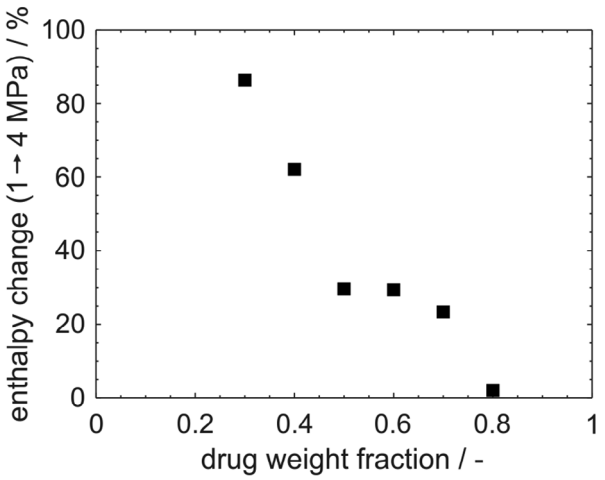

Figure 8. Enthalpy change of the drug dissolution of ACE in PVPVA from 1 to 4 MPa CO_{2-} pressure and at a heating rate of 10 °C min^{-1}.

When comparing the slope of the extrapolation at 1 and 4 MPa CO_{2-} pressure for the ACE/PVPVA formulation (**Figure 9**), it is noticeable that this decreases with higher pressure for drug weight fractions from 40 to 100 wt.%. As previously described, the lower gradient characterizes the higher diffusion coefficient

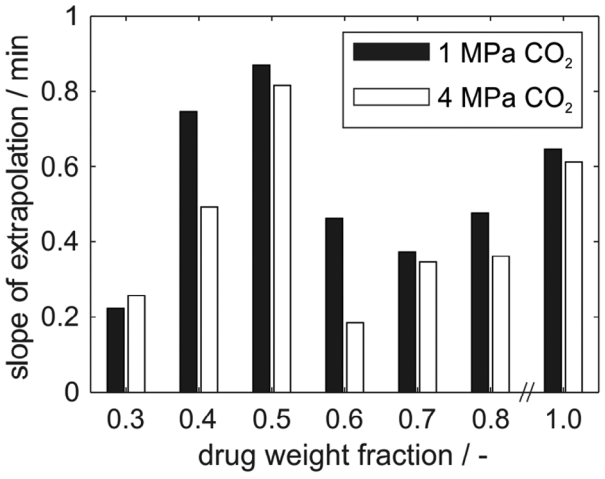

Figure 9. The slope of the extrapolation to a zero heating rate of ACE/PVPVA at 1 and 4 MPa CO_{2-} pressure.

of the drug in the polymer under elevated CO_{2-} pressure. Here, the diffusion is accelerated by the dissolved CO_2 that plasticizes the polymer and leads to an increase in free volume. As a result, the drug diffuses in a less hindered manner in the polymer than in the absence of CO_2 or at lower CO_2 fractions.[33]

A consistent course of the slope of extrapolation over the drug fraction was not determined. However, a decrease in the gradient with higher CO_2 pressure was found for all compositions, except for that with the drug weight fraction of 30 wt.%. Here, a slight increase in the gradient was detected.

4. Conclusion

The influence of CO_2 on drug-polymer phase behavior was investigated utilizing high-pressure DSC measurements. Therefore, quasi-binary phase diagrams at different CO_{2-} pressures were evaluated for four ASD formulations. Plastification already occurs at lower temperatures when CO_2 is dissolved since the specific volume is increased and intermolecular interactions are weakened so that the glass transition temperature is reduced. The strength of this effect depends on the spatial and chemical structure of the components. Furthermore, the sorption of CO_2 accelerates the diffusion of the drug in the plasticized polymer. The energy required to dissolve the drug in the polymer decreases under CO_2 due to its effect on the bonds in the crystalline structure of the drug. On the one hand, there was a slight decrease in the solubility temperature of the drug in the polymer which means that the CO_2 promotes the dissolution of a larger amount of drug at a certain temperature. On the other hand, phase separation was detected in some formulations under CO_2 which could have an impact on the stability of the ASD formulations during storage.

Supporting Information

Supporting Information is available from the Wiley Online Library or from the author.

Acknowledgements

The authors appreciate the generous donation of Soluplus by BASF SE.
Open access funding enabled and organized by Projekt DEAL.

Conflict of Interest

The authors declare no conflict of interest.

Data Availability Statement

The data that support the findings of this study are available from the corresponding author upon reasonable request.

Keywords

carbon dioxide, formulation design, glass transition, phase diagrams, phase separation, solubility

Received: September 24, 2024
Revised: November 13, 2024
Published online: November 29, 2024

[1] A. Schittny, J. Huwyler, M. Puchkov, *Drug Deliv.* **2020**, *27*, 110.
[2] M. Rodriguez-Aller, D. Guillarme, J.-L. Veuthey, R. Gurny, *J. Drug Deliv. Sci. Technol.* **2015**, *30*, 342.
[3] a) J. Winck, T. Gottschalk, M. Thommes, *Pharmaceutics* **2023**, *15*, 1417; b) J. Winck, M. Daalmann, A. Berghaus, M. Thommes, *Pharm. Dev. Technol.* **2022**, *27*, 1009.
[4] a) S. Baghel, H. Cathcart, N. J. O'Reilly, *J. Pharm. Sci.* **2016**, *105*, 2527; b) J. S. LaFountaine, J. W. McGinity, R. O. Williams, *AAPS Pharm. Sci. Tech.* **2016**, *17*, 43.
[5] A. Kasturirangan, C. A. Koh, A. S. Teja, *Ind. Eng. Chem. Res.* **2011**, *50*, 158.
[6] I. Kikic, F. Vecchione, P. Alessi, A. Cortesi, F. Eva, N. Elvassore, *Ind. Eng. Chem. Res.* **2003**, *42*, 3022.
[7] U. A. Handge, V. Altstädt, *J. Rheol.* **2012**, *56*, 743.
[8] E. Kiran, J. A. Sarver, J. C. Hassler, *J. Supercrit. Fluids* **2022**, *185*, 105378.
[9] X. Zhang, S. Heinonen, E. Levänen, *RSC Adv.* **2014**, *4*, 61137.
[10] B. Subramaniam, R. A. Rajewski, K. Snavely, *J. Pharm. Sci.* **1997**, *86*, 885.
[11] G. Verreck, A. Decorte, K. Heymans, J. Adriaensen, D. Liu, D. Tomasko, A. Arien, J. Peeters, G. van den Mooter, M. E. Brewster, *Int. J. Pharm.* **2006**, *327*, 45.
[12] a) G. P. Andrews, O. Abu-Diak, F. Kusmanto, P. Hornsby, Z. Hui, D. S. Jones, *J. Pharm. Pharmacol.* **2010**, *62*, 1580; b) Z. K. Nagy, M. Sauceau, K. Nyúl, E. Rodier, B. Vajna, G. Marosi, J. Fages, *Polym. Adv. Technol.* **2012**, *23*, 909.
[13] a) J. G. Lyons, M. Hallinan, J. E. Kennedy, D. M. Devine, L. M. Geever, P. Blackie, C. L. Higginbotham, *Int. J. Pharm.* **2007**, *329*, 62; b) G. Verreck, A. Decorte, H. Li, D. Tomasko, A. Arien, J. Peeters, P. Rombaut, G. van den Mooter, M. E. Brewster, *J. Supercrit. Fluids* **2006**, *38*, 383.
[14] a) G. Verreck, A. Decorte, K. Heymans, J. Adriaensen, D. Liu, D. L. Tomasko, A. Arien, J. Peeters, P. Rombaut, G. van den Mooter, M. E. Brewster, *J. Supercrit. Fluids* **2007**, *40*, 153; b) G. Verreck, A. Decorte, K. Heymans, J. Adriaensen, D. Cleeren, A. Jacobs, D. Liu, D. Tomasko, A. Arien, J. Peeters, P. Rombaut, G. van den Mooter, M. E. Brewster, *Eur. J. Pharm. Sci.* **2005**, *26*, 349.
[15] S. K. Rahimi, K. O'Donnell, B. Haight, A. Machado, C. Martin, F. Meng, T. Listro, F. Zhang, *J. Pharm. Sci.* **2021**, *110*, 1444.
[16] M. Almutairi, B. Almutairy, S. Sarabu, A. Almotairy, E. Ashour, S. Bandari, A. Batra, D. Tewari, T. Durig, M. A. Repka, *J. Drug Deli. Sci. Technol.* **2019**, *52*, 165.
[17] E. A Ashour, V. Kulkarni, B. Almutairy, J.-B. Park, S. P. Shah, S. Majumdar, Z. Lian, E. Pinto, V. Bi, T. Durig, S. T. Martin, M. A. Repka, *Drug Dev. Ind. Pharm.* **2016**, *42*, 123.
[18] D. L. Tomasko, H. Li, D. Liu, X. Han, M. J. Wingert, L. J. Lee, K. W. Koelling, *Ind. Eng. Chem. Res.* **2003**, *42*, 6431.
[19] R. Obaidat, M. Alnaief, P. Jaeger, *Pharm. Dev. Technol.* **2018**, *23*, 697.
[20] C. Potter, Y. Tian, G. Walker, C. McCoy, P. Hornsby, C. Donnelly, D. S. Jones, G. P. Andrews, *Mol. Pharm.* **2015**, *12*, 1377.
[21] S. Milovanovic, J. Djuris, A. Dapčević, D. Medarevic, S. Ibric, I. Zizovic, *Polym. Test.* **2019**, *76*, 54.
[22] A. Prudic, Y. Ji, G. Sadowski, *Mol. Pharm.* **2014**, *11*, 2294.
[23] D. E. Moseson, L. S. Taylor, *Int. J. Pharm.* **2018**, *553*, 454.
[24] K. Lehmkemper, S. O. Kyeremateng, O. Heinzerling, M. Degenhardt, G. Sadowski, *Mol. Pharm.* **2017**, *14*, 157.
[25] R. Nair, N. Nyamweya, S. Gönen, L. J. Martínez-Miranda, S. W. Hoag, *Int. J. Pharm.* **2001**, *225*, 83.
[26] F. Wolbert, I.-K. Fahrig, T. Gottschalk, C. Luebbert, M. Thommes, G. Sadowski, *Pharmaceutics* **2022**, *14*, 269.
[27] K. Six, G. Verreck, J. Peeters, M. Brewster, G. van den Mooter, *J. Pharm. Sci.* **2004**, *93*, 124.

[28] M. A. Altamimi, S. H. Neau, *Drug Dev. Ind. Pharm.* **2016**, *42*, 446.
[29] T. Gottschalk, C. Özbay, T. Feuerbach, M. Thommes, *Pharmaceutics* **2022**, *14*, 1757.
[30] M. Kargar, U. A. Handge, *Macro Theory Simul.* **2021**, *30*, 2100016.
[31] Y. Sun, J. Tao, G. G. Z. Zhang, L. Yu, *J. Pharm. Sci.* **2010**, *99*, 4023.
[32] G. Höhne, W. Hemminger, H.-J. Flammersheim, *Differential Scanning Calorimetry: An Introduction for Practitioners*, Springer, Berlin, Heidelberg **2003**.
[33] S. G. Kazarian, N. H. Brantley, B. L. West, M. F. Vincent, C. A. Eckert, *Appl. Spectrosc.* **1997**, *51*, 491.
[34] a) A. H. Al-Marzouqi, I. Shehatta, B. Jobe, A. Dowaidar, *J. Pharm. Sci.* **2006**, *95*, 292; b) J. Karimi Sabet, C. Ghotbi, F. Dorkoosh, A. Striolo, *Scient. Iranica* **2012**, *19*, 619; c) R. D. Oparin, A. Idrissi, M. V. Fedorov, M. G. Kiselev, *J. Chem. Eng. Data*. **2014**, *59*, 3517.
[35] J. Klueppelberg, U. A. Handge, M. Thommes, J. Winck, *Pharmaceutics.* **2023**, *15*, 2650.
[36] M. F. Kemmere, T. Meyer, *Supercritical Carbon Dioxide in Polymer Reaction Engineering*, Wiley-VCH, Weinheim, Great Britain **2010**.
[37] C. Brütting, J. Dreier, C. Bonten, V. Altstädt, H. Ruckdäschel, *J. Cell. Plast.* **2022**, *58*, 917.
[38] J. T. Reilly, C. P. Bokis, M. D. Donohue, *Int. J. Thermophys.* **1995**, *16*, 599.
[39] F. Harden, M. Kargar, U. A. Handge, *Adv. Polym. Technol.* **2022**, *2022*, 1.
[40] D. Liu, *Thermodynamic, and Glass Transition Behavior in CO_2–Polymer Systems Emphasizing the Surface Region, Dissertation*, The Ohio State University, Columbus, OH **2006**.
[41] a) X. Luo, S. Xie, J. Liu, H. Hu, J. Jiang, W. Huang, H. Gao, D. Zhou, Z. Lü, D. Yan, *Polym. Chem.* **2014**, *5*, 1305; b) A. Khalyavina, L. Häußler, A. Lederer, *Polymer* **2012**, *53*, 1049.
[42] G. Li, F. Gunkel, J. Wang, C. B. Park, V. Altstädt, *J. Appl. Polym. Sci.* **2007**, *103*, 2945.
[43] K. Six, H. Berghmans, C. Leuner, J. Dressman, K. van Werde, J. Mullens, L. Benoist, M. Thimon, L. Meublat, G. Verreck, J. Peeters, M. Brewster, G. van den Mooter, *Pharm. Res.* **2003**, *20*, 1047.
[44] M. Škerget, Ž. Knez, M. Knez-Hrnčič, *J. Chem. Eng. Data.* **2011**, *56*, 694.
[45] S. K. Shukla, J.-P. Mikkola, *Phys. Chem. Chem. Phys. : PCCP* **2018**, *20*, 24591.

